Summer 2012

Rotating-shield brachytherapy (RSBT) for cervical cancer

Wenjun Yang
University of Iowa

ROTATING-SHIELD BRACHYTHERAPY (RSBT) FOR CERVICAL CANCER

by

Wenjun Yang

A thesis submitted in partial fulfillment
of the requirements for the Master of
Science degree in Biomedical Engineering
in the Graduate College of
The University of Iowa

July 2012

Thesis Supervisor: Assistant Professor Ryan T. Flynn

Graduate College
The University of Iowa
Iowa City, Iowa

CERTIFICATE OF APPROVAL

_____

MASTER'S THESIS

_____

This is to certify that the Master's thesis of

Wenjun Yang

has been approved by the Examining Committee
for the thesis requirement for the Master of Science
degree in Biomedical Engineering at the July 2012 graduation.

Thesis Committee: _____
Ryan T. Flynn, Thesis Supervisor

_____
Joseph M. Reinhardt

_____
John E. Bayouth

_____
Yusung Kim

ACKNOWLEDGEMENTS

I would like to give my sincere thanks to all who help me to finish this thesis: To Ryan Flynn for his direction, patience and the great support throughout my master study. To Yusung Kim for his generous help on the clinical knowledge and suggestions on my manuscript. To Xiaodong Wu for his instructions on the algorithms to lead our research to go deeper. To Yunlong Liu and Xing Li, for their cooperation and making the study a happy time. To my parents, for their great encouragement no matter I'm scoring 100 or 0. To my fiancee, Yan Zhang, for letting me know what's really important.

ABSTRACT

Purpose: To assess rotating shield brachytherapy (RSBT) delivered with electronic brachytherapy (eBT) sources compared to intracavitary (IC) and intracavitary plus supplemental interstitial brachytherapy (IC+IS BT) delivered with a conventional ^{192}Ir source.

Method and Materials: An in-house treatment planning system (TPS) for RSBT was developed, and IC, IC+IS and RSBT treatment plans were simulated for 5 patients with bulky (>40cc) advanced cervical cancer high-risk target volumes (HR-CTVs). All treatment planning was based on magnetic resonance (MR) images with HR-CTV, bladder, rectum, and sigmoid colon contouring done by a radiation oncologist. A bio- and MRI-compatible polycarbonate (Makrolon Rx3158) intrauterine applicator was simulated for IC and RSBT, and the Vienna applicator was simulated for IC+IS BT. ^{192}Ir was used as the radiation source of IC and IC+IS BT, and the Xoft Axxent^{TM} eBT source was used for RSBT. A 0.5 mm thick tungsten shield was used for RSBT. Two shield models, with azimuthal 45°, zenith 180° (RSBT-45) and azimuthal 180°, zenith 180° (RSBT-180) was selected in this study. BT planning was done by escalating: maximizing HR-CTV dose without exceeding bladder, rectum, and sigmoid dose tolerances. The total dose for each plan included both the external beam radiation therapy (EBRT) and BT doses.

Results: The minimal dose of the hottest 90% of HR-CTV volume (D90) and treatment time was selected as the metric of plan evaluation. RSBT and IC+IS BT had higher D90 than IC BT for all 5 patients. For RSBT-180/IC+IS, the D90 ratio ranged from 66% to 100%, with average of 86%; the treatment time ratio ranged from 137% to 208%, with average of 169%. For RSBT-45/IC+IS, the D90 ratio ranged from 101% to

123%, with the average of 113%; the treatment time ratio ranged from 749% to 1188%, with the average of 907%.

Conclusions: RSBT for advanced cervical cancer can provide variant D90 and treatment time with different azimuthal angles. For RSBT-45, the D90 was improved at the cost of increased treatment time. For RSBT-180, the treatment time was strictly controlled but D90 was not guaranteed. There will be an angle to achieve the balance of D90 and treatment time.

TABLE OF CONTENTS

LIST OF TABLES VI

LIST OF FIGURES VII

CHAPTER 1 INTRODUCTION 1
1.1 Cervical cancer 1
1.2 Standard of care for cervical cancer 2
1.3 Brachytherapy 3
1.4 Rotating-shield brachytherapy 4
1.5 Rationale of our study 4

CHAPTER 2 MATERIALS AND METHODS 6
2.1 Treatment planning system (TPS) of RSBT 6
2.2 Patients and dose prescriptions 8
2.2 Radiation Source and applicator 9
2.3 Delivery technique 12
2.4 Dose calculation 15
2.5 Optimization methods 16
2.6 Evaluation metric 17

CHAPTER 3 RESULTS 18
3.1 D90 and treatment time statistics 18
3.2 DVH curve 18
3.3 Dose distribution map 19
3.4 Effect of azimuthal angle 21
3.5 Effect of zenith angle 22

CHAPTER 4 DISCUNSSION AND CONCLUSION 23

REFERENCES 25

LIST OF TABLES

Table 1-1. Local control and survival rate by stage.....2

Table 2-1. The terminologies defined in RS-IMBT.....13

Table 2-2. Variables of modified-TG-43 dose calculation equation 15

Table 2-3. Main variables defined in the optimization equation 17

LIST OF FIGURES

Figure 1-1. Vienna applicator for IC+IS and IC BT 3

Figure 1-2. BrachyVision, the BT planning system used at UIHC 5

Figure 2-1. Flow chart of the in-house TPS for RSBT 6

Figure 2-2. Geometry of MRI image slice and patient position 7

Figure 2-3. Physician delineated contour for the bladder of patient 1 7

Figure 2-4. MRI image and reconstructed 3D structure for HR-CTV and OAR 8

Figure 2-5. Geometry design of the RSBT shield 10

Figure 2-6. Shield open area with different azimuth and zenith angles 11

Figure 2-7. RSBT coordinate system for dose calculation and shield rotating&moving 12

Figure 2-8. RSBT source with shield rotating and shifting process. 14

Figure 3-1. D90 and treatment time comparison between RSBT and IC+IS BT 18

Figure 3-2. DVH of 5 patients with RSBT-180, RSBT-45, IC and IC+IS BT 19

Figure 3-3. Dose distribution map for 5 patients with IC, IC+IS, RSBT-180 and RSBT-45 20

Figure 3-4. RSBT parameter selection curve 21

CHAPTER 1

INTRODUCTION

1.1 Cervical cancer

Cervical cancer is a malignant neoplasm of the cervix uteri or cervical area. It is the leading cause of cancer mortality in women in developing countries and third most common gynecological cancer in the US [1]. One of the most common symptoms of cervical cancer is abnormal vaginal bleeding, but there may be no symptoms in the early stages [2, 3].

More than 90% of cervical cancer is caused by Human papillomavirus (HPV) infection [3, 4]. Not all of the causes of cervical cancer are known, and several other contributing factors include smoking [5] chlamydia infection, stress and stress-related disorders, dietary factors, hormonal contraception, multiple pregnancies, exposure to the hormonal drug diethylstilbestrol, and family history of cervical cancer [6].

In 2011, more then 12,000 newly diagnosed cervical cancer cases were reported in the U.S., with the death rate of about 33.8% [7]. The death rate is related to the cancer stage, which is shown in Table 1. Cervical cancer cases of stage IB2 to stage IV were studied in this work since these advanced-staged cancer cases tend to receive brachytherapy and have bulky volume (>40cc) to benefit from our treatment method.

Table 1-1 [1]. Local control and survival rate by stage

Local control rate		5 years survival	
IA	95-100%	IA	95-100%
IB1	90-95%	IB2	85-90%
IB2	60-80%	IB2	60-70%
IIA	80-85%	IIA	75%
IIB	60-80%	IIB	60-65%
IIIA	60%	IIIA	25-50%
IIIB	50-60%	IIIB	25-50%
IVA	30%	IVA	15-30%
		IVB	<10%

1.2 Standard of care for cervical cancer

Early stages (IB1 and IIA less than 4 cm) can be treated with radical hysterectomy with removal of the lymph nodes or radiation therapy. Radiation therapy is given as external beam radiotherapy to the pelvis and brachytherapy (internal radiation). Patients treated with surgery who have high risk features found on pathologic examination are given radiation therapy with or without chemotherapy in order to reduce the risk of relapse [1].

Larger early stage tumors (IB2 and IIA more than 4 cm) may be treated with radiation therapy and cisplatin-based chemotherapy, hysterectomy (which then usually requires adjuvant radiation therapy), or cisplatin chemotherapy followed by hysterectomy [1].

Advanced stage tumors (IIB-IVA) are treated with radiation therapy and cisplatin-based chemotherapy [1].

1.3 Brachytherapy

Brachytherapy (BT) plays a crucial role in the treatment of invasive cervical cancer from stage I to IV, especially in advanced stage (IB2 or higher) [8, 9]. It is an intracavitary (IC) high-dose-rate (HDR) radiation therapy, delivering much higher dose per fraction than external beam radiotherapy (EBRT) to the target tumor volume without violating the organs at risk (OAR) toxicity threshold because of the very high dose gradient around the source (about 10% per mm) [9]. Conventionally, a radiation source with a radially symmetric dose distribution is used in brachytherapy. As a result, the OAR around the cervical cancer, such as bladder, sigmoid and rectum restrict the radiation dose that can be delivered to the non-symmetric extensions of bulky (>4 cm) tumors [10]. To compensate for the sometimes poor conformance of the intracavitary-only dose distribution, needle-based intracavitary plus interstitial (IC+IS) BT is can be used [8-14]. Figure 1-1 is one example of the applicator used in IC and IC+IS BT.

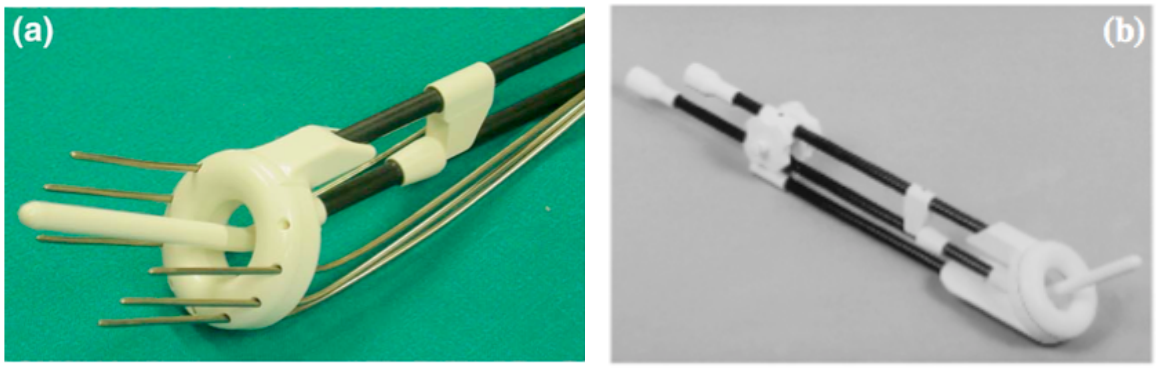

Figure 1-1. Vienna applicator for IC+IS and IC BT. (a) Vienna applicator with ring and needle [11], (b) Stockholm based intracavitary applicator [15]

1.4 Rotating-shield brachytherapy

Rotating shield brachytherapy (RSBT) was conceptually proposed by Ebert in 2002 [16]. It delivered the dose through a partially shielded radiation source in an optimized step-shot fashion to improve tumor dose conformity. It's a type of intensity-modulated brachytherapy (IMBT) in which the amount of time the shield is pointed in a given direction is controlled. RSBT may be less invasive than interstitial BT since there is no need of needles, and the extra time for setting up interstitial applicator is spared. With the electronic radiation source which is with relatively low energy (26 keV on average), RSBT enables clinical staff to be in the treatment room during delivery, and would eliminate the need for an expensive shielded room for conventional BT. Thus patients could be treated in a room next to the MRI or CT room, reducing the added complexity of transporting patients between the BT suite and the imaging room. Other groups have studied the theoretical effectiveness of RSBT for prostate [17] and breast [18] cancer.

1.5 Rationale of our study

In this work, we proposed to apply RSBT with electronic source for cervical cancer with bulky (>40cc) volume. With the relatively low source energy (average 26ev), we could use 2mm-thick tungsten shield which can be placed into the IC BT applicator. We also developed a treatment planning system for RSBT to compare the treatment result with conventional IC and IC+IS BT.

Commercially available HDR-BT planning systems of which we are aware are capable of IC+IS BT. Figure 1-2 is the user interface of BrachyVision, the BT planning system used at the University of Iowa Hospitals and Clinics (UIHC). From this planning

system, we can check different slices of the patient MRI image, high-risk clinical target volume (HR-CTV) of cervical cancer, OAR and applicator position, and different dose coverage. This system is for conventional IC or IC+IS only. In this work we developed an in-house RSBT treatment planning system (TPS) for cervical cancer. The TPS generates RSBT optimized dose distributions based on patient image data exported from BrachyVision, and is capable of dose and dose-volume histogram (DVH) display for treatment plan evaluation.

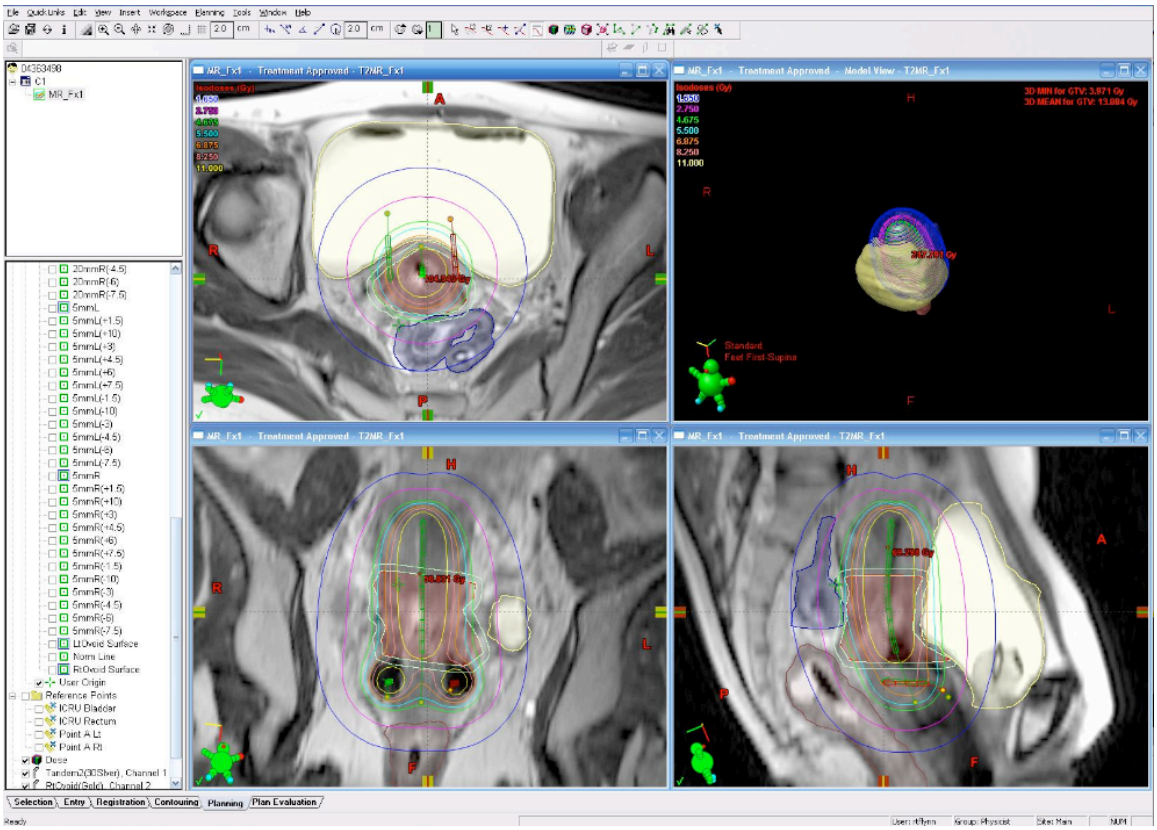

Figure 1-2. BrachyVision, the BT planning system used at UIHC

CHAPTER 2

MATERIALS AND METHODS

2.1 Treatment planning system (TPS) of RSBT

The flow chart of our in-house TPS is shown in figure 2-1. The TPS was developed in the Matlab programming environment. For the first step in the treatment planning process, an image reading tool was developed to read in the patient MR image and the contour data of HR-CTV and OAR from DICOM files exported from BrachyVision. Since the MRI image was acquired with a rotation angle, α, along the X axis, a simple image transform (rotation and translation) is necessary to align the image slice with the physical MRI slice, as shown in figure 2-2.

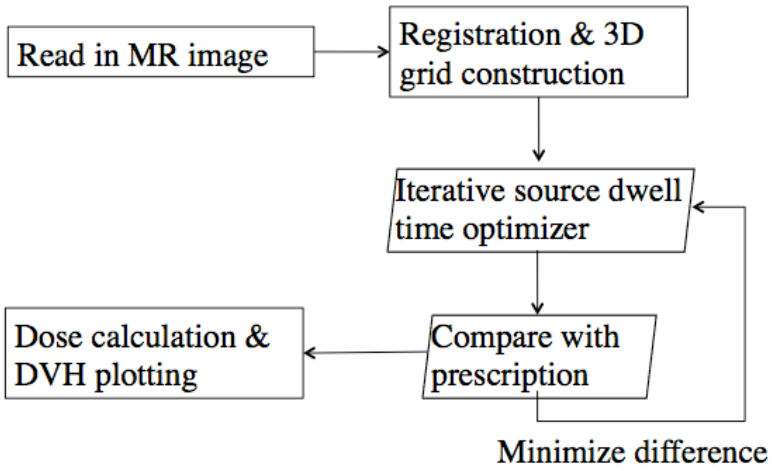

Figure 2-1. Flow chart of the in-house TPS for RSBT

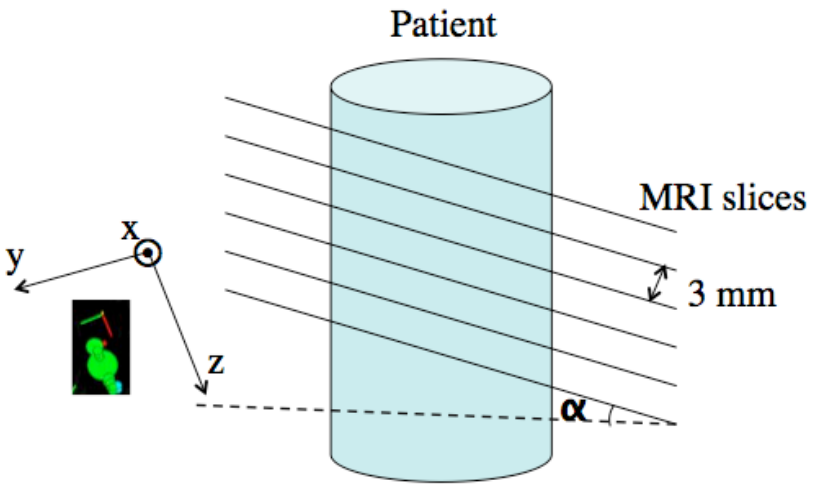

Figure 2-2. Geometry of MRI image slice and patient position

The image rotation matrix of α is stored in the header of the DICOM file, and the image registration is achieved by multiplying the image coordinates by the inverse rotation matrix. The figure 2-3 shows the bladder contour before and after registration.

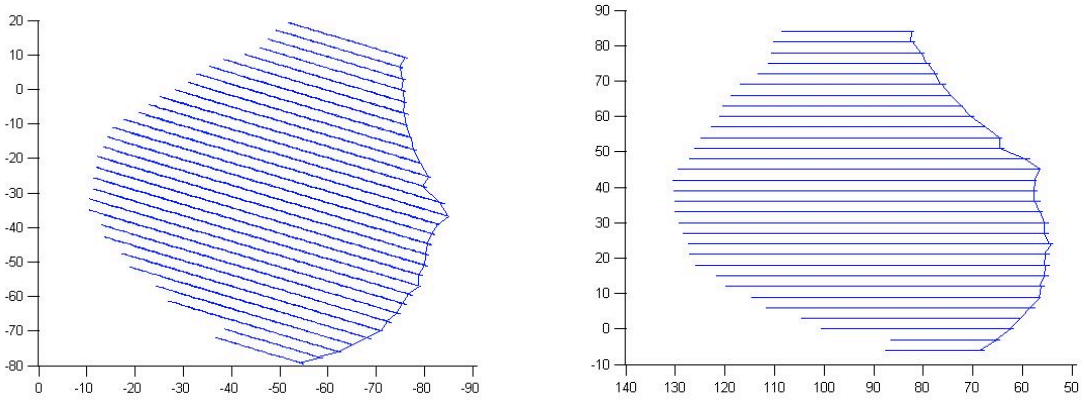

(a) (b)

Figure 2-3. Physician delineated contour for the bladder of patient 1. (a) The bladder contour before registration, (b) The bladder contour after registration

The images after registration were used to construct the 3D grid for dose calculation. As shown in figure 2-4, the binary masks for HR-CTV and OAR were constructed. And then the space relationship can be founded between the applicator and the volumes.

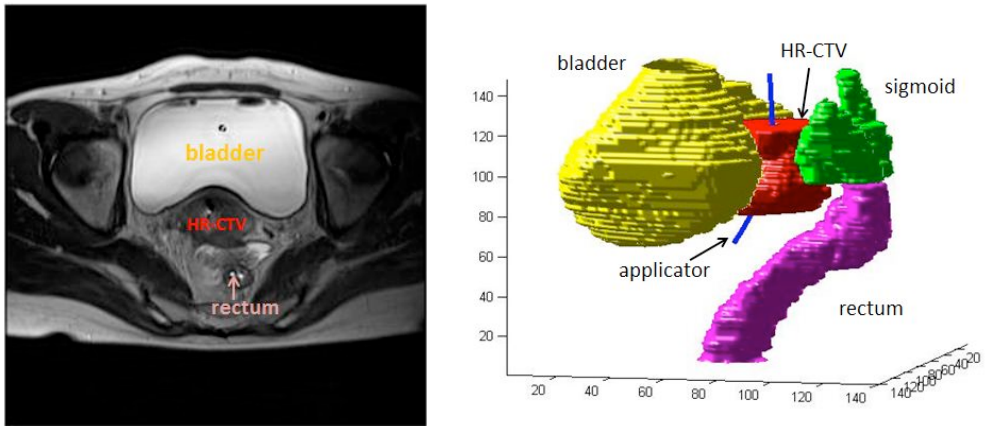

(a) (b)

Figure 2-4. MRI image and reconstructed 3D structure for HR-CTV and OAR. (a) Transverse MRI of cervical cancer and adjacent organs, (b) Reconstructed 3D binary masks of tumor and OARs

The cervical cancer cases, materials, and the dose optimization and calculation mechanism will be discussed in the following sections.

2.2 Patients and dose prescriptions

Five patients with biopsy-confirmed cervical cancer (treated from 2009 to 2010) having large high risk CTV (HR-CTV) were selected based on the tumor volume (>40cc) and shape. Large HR-CTV cases were selected because we found that even the MRI-guided, conformal HDR-BT technique was limited to provide proper dose-HR-CTV conformity. And so such cases need IC+IS BT to provide better dose-tumor coverage,

which will benefit from RSBT [8]. The cancer International Federation of Gynecology and Obstetrics (FIGO) stage ranged from IB to IVA, with lymph node and parametrial involvement and maximum dimension greater than 4 cm. Curative radiation therapy (RT) was performed, consisting of external beam RT with concomitant chemotherapy followed by HDR-BT (5.5 Gy per fraction with 5 fractions). To cover parametrial regions, an EBRT boost (5.4 Gy with 1.8 Gy fraction size) was performed. High-resolution (3.0 Tesla) MR images were acquired with a Siemens MAGNETOM Trio 3T MR scanner (Siemens Medical Solutions, Erlangen, Germany). HR-CTV and OAR that clinically delineated (using GEC-ESTRO guidelines [8]) on T2-weighted MRI were retrospectively imported into the in-house TPS. Clinically reconstructed source-pathway information of a tandem was imported into an applicator-source-pathway. The detail of MRI scanning protocol and scanning method, such as 'Brachytherapy Eye View' was reported in our previous study.

One BT plan was assumed to be repeated during subsequent BT fractions. The MRI images were acquired from the first fraction. The linear-quadratic parameters used were: $\alpha/\beta = 3$ Gy for OAR and $\alpha/\beta = 10$ Gy for tumor [19]. The final dose result was the summation of EBRT and dose/fraction multiplied by fraction number in BT. We used the OAR dose constraints of D2cc $\leq$ 75 Gy_3 for rectum and sigmoid, D2cc $\leq$ 90 Gy_3 for bladder, which is consistent with that used by other groups [9, 20].

2.2 Radiation Source and applicator

For RSBT, we simulated the same applicator as that in intracavitary BT as shown in figure 1-1. We proposed an electronic radiation source, Xoft Axxent^{TM} for RSBT, since with the relatively low energy (26.8 keV), only 0.5 mm thick tungsten shield is

needed to reduce the transmission to less than 0.1%. According to Ebert's study [16], the more transmission, the poorer dose conformity can be achieved. In our study, we assumed the shield was rotated along the curved axis of the applicator.

There are two other reason why we selected the Xoft Axxent™ (Xoft Inc., Sunnyvale, CA) miniature x-ray (photon) tube as the radiation source for RSBT. First, its dose rate in water at 2 cm lateral to the source axis is greater than 1 Gy/min, which is comparable to that of ^{192}Ir BT, preventing a significant treatment time increase for RS-IMBT. Second, the transmission of the low energy (26.8 keV average) photons emitted by the eBT source can be reduced to 0.1% with only 0.5mm of tungsten shield. Over 2 cm of gold or tungsten would be required to achieve a similar shield transmission for ^{192}Ir photons, which is too much to fit inside an intracavitary uterine applicator.

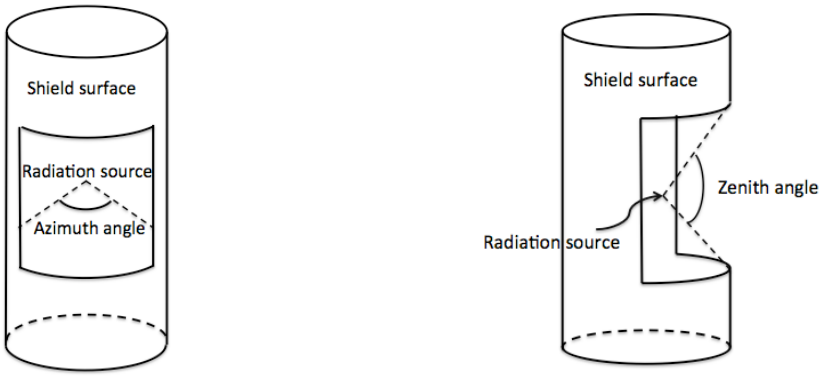

Figure 2-5. Geometry design of the RSBT shield. (a) Front view, with the azimuthal angle defined window width (b) Side view, with the zenith angle defined window height. Radiation source is placed at the center of the shield, and the azimuth and zenith angle define the window size. The line-shape radiation source is simulated as a point

As shown in figure 2-5, a 0.5 mm thick shield made of tungsten was applied around the radiation source to modify the intensity. With different shield azimuth and zenith angle, the dose shape could be modified. In conventional BT with ^{192}Ir, no shield was used.

The dose distribution is illustrated as figure 2-6. The source was simulated as a point source and the shield open area is modulated by the azimuthal and zenith angle. In the following sections, all the dose distribution will be illustrated as pyramid shape. In this work, we assumed shield photon transmission was zero. It is ignorable at the tumor edge, which is the key parameter of the emission time optimization.

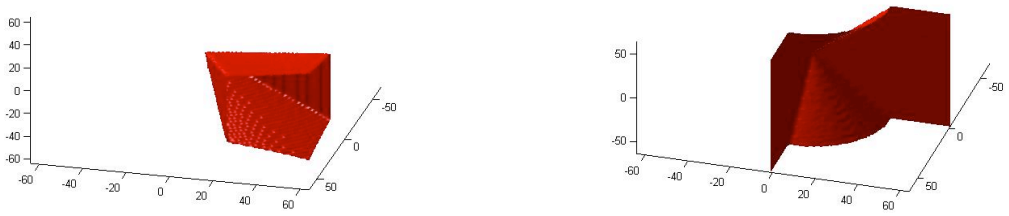

(a) (b)

Figure 2-6. Shield open area with different azimuth and zenith angles. (a) azimuth angle = 45°, zenith angle = 45°, (b) azimuth angle = 90°, zenith angle = 120°

2.3 Delivery technique

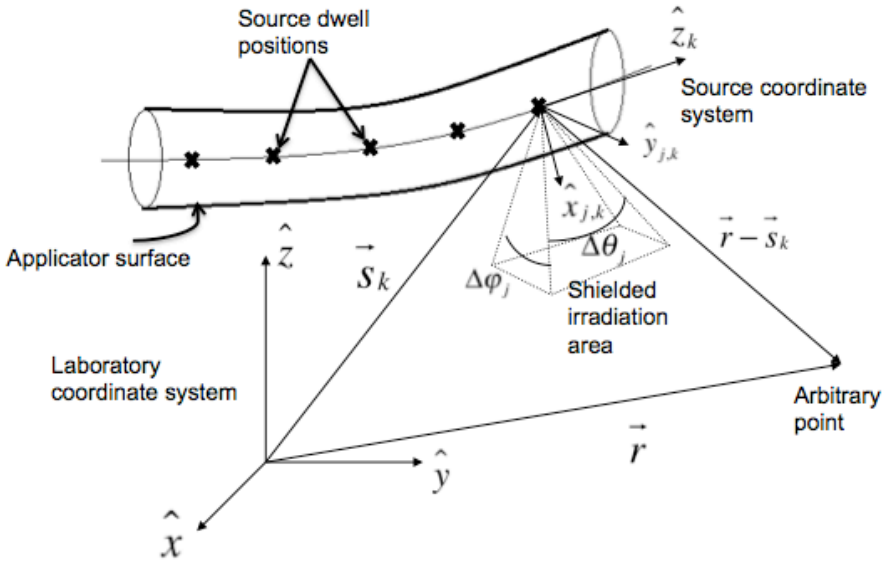

Figure 2-7. RSBT coordinate system for dose calculation and shield rotating&moving. The eBT source is placed in the applicator positions sequentially. The dashed pyramid indicates the azimuthal and zenith shield emission angles. Every point in the space is defined in two coordinate systems: the laboratory and source coordinate system. The shield is rotated along z'_k. The dwell time of each position is optimized using a linear least square optimization technique. After a full rotation at one dwell position, the source moves to the next one and the process is repeated.

As shown in figure 2-7, the radiation source was simulated to be placed at the dwell positions sequentially within the applicator. At each dwell position, the radiation source was rotated around z'_k. The number of emission per dwell position can be specified by the user. The emission time was optimized with a linear least square optimizer such that the dose distribution would conform to the tumor shape. The source moved to the next dwell position and repeated this process after a 360° rotation.

Table 2-1. The terminologies defined in RS-IMBT

Dwell position	The stop positions of the radiation source within the applicator
Emission	Dose delivery at each dwell position. The number of emissions at each dwell position as shield rotating is set by user
n	The number of dwell positions in one RS-IMBT treatment
N	The number of emissions at each dwell position
j	The index of emissions. If there are 16 emissions at each dwell position, each emission is indexed with j = 0…15
$\Delta\gamma$	The emission step angle, which is the angle the shield travelled between emission j and j+1. $\Delta\gamma = 2\pi/N$
γ_j	The angle between the current shield central line and that of emission j = 0. $\gamma_j = j\Delta\gamma$, where j = 0…N-1
$\Delta\varphi$	The shield azimuthal angle, as shown in figure 2-5 (a). $\min(\Delta\varphi) = \Delta\gamma$, such that there isn't any cold point not covered between each emission.
$\Delta\theta$	The shield zenith angle, as shown in figure 2-5 (b). The number of dwell position, n is determined by $\Delta\theta$, such that there isn't any cold position between each dwell position.

In this study, we specified n = 8 and N = 16. With 8 dwell positions, the distance between each one is about 5 mm, which is a typical value in clinical situations. The number of 16 emissions provided a fine enough intensity-modify resolution.

We used different shield azimuth angle, $\Delta\varphi$, from 45° to 180° in out study. Since N = 16, $\pi/8$ is the minimal value allowed ($\min(\Delta\varphi) = \Delta\gamma = 360°/N$). In this case as shown in figure 2-8 (a), it's a non-overlapping rotation: at emission j = 4 and j = 5, the shield covered and only just covered that area, with no overlapping. While with larger $\Delta\varphi$ ($\Delta\varphi > \Delta\gamma$) as shown in figure 2-8 (b), there is an overlapping between each emission, such as j = 4 and j = 5.

We also used different shield zenith angle, $\Delta\theta$, from 90° to 180°. Figure 2-8 (c) and 2-8 (d) shows the relationship between the dwell position distance and $\Delta\theta$.

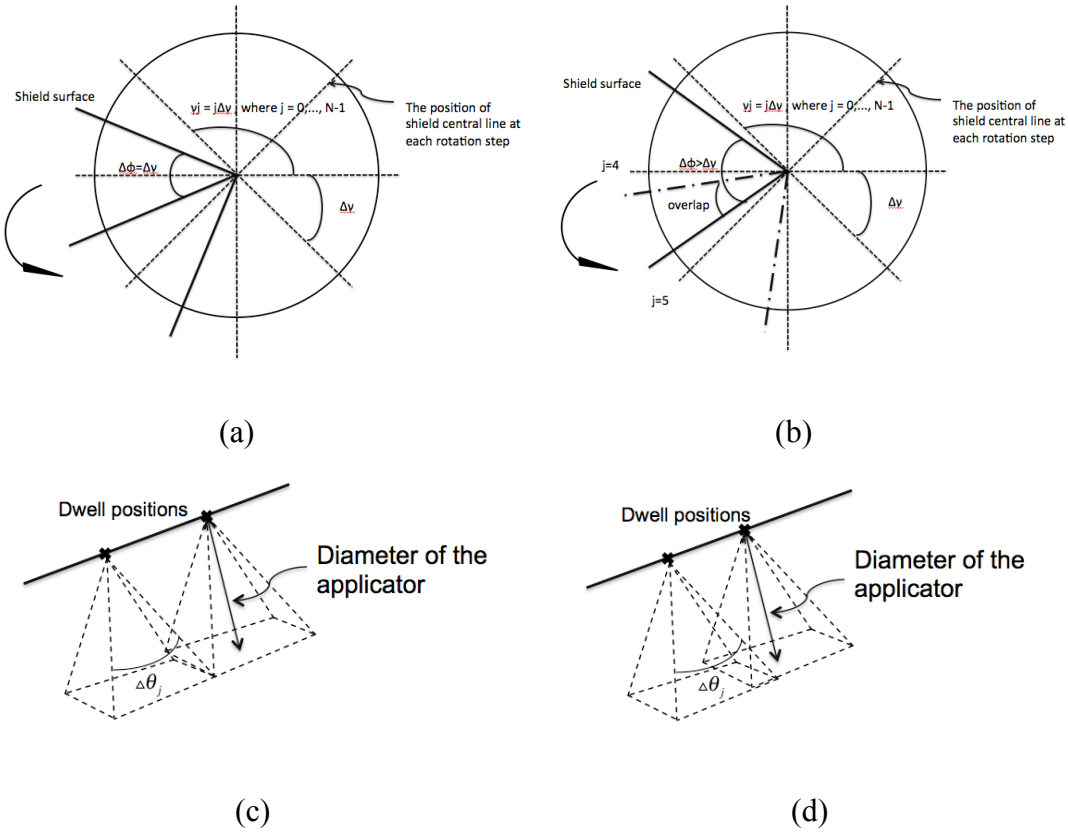

Figure 2-8. RSBT source with shield rotating and shifting process (a) the shield azimuth angle is equal to the rotation step angle, so that there isn't overlap between each rotation, (b) The shield azimuth angle is greater than the rotation step angle, which brings overlap between each rotation, (c) The minimal zenith angle is shown such that there won't be any cold points outside the applicator, (d) The zenith angle is larger so there will be overlap between dwell positions.

Two azimuthal angle shields (45° and 180°) with constant zenith angle (180°) were applied to all the 5 patients. They are called RSBT-45 and RSBT-180. These two angles were selected to represent fine and broad azimuthal shield angles, and are not expected to be optimal choices. More shield model with different azimuthal and zenith angle was applied only to patient 1, to investigate the effect of azimuthal and zenith angle.

2.4 Dose calculation

The TG-43 method was used for dose calculation, and the medium through which the photons transmitted was assumed to be water.

$$\dot{D}_{j,k}(\vec{r},\Delta\phi_s,\Delta\theta_s) = S_k \Lambda \frac{G_k(\vec{r})}{G_k(\vec{r}_0)} g(|\vec{r}-\vec{s}_k|)\ F_k(\vec{r})\ T_{j,k}(\vec{r},\Delta\phi_s,\Delta\theta_s)$$

Equation1 Modified-TG-43 equation for dose calculation

The definition of each function in equation 1 and the corresponding approximated functions are shown in table 2.

Table 2-2. Variables of modified-TG-43 dose calculation equation

$\dot{D}_{j,k}(\vec{r},\Delta\phi_s,\Delta\theta_s)$	Dose rate of any point of jth dwell position and kth emission in the laboratory coordinate system. It depends on the position $\vec{r}$, the azimuth angle $\Delta\phi_s$, and the zenith angle $\Delta\theta_s$ of the shield.
S_k	Air strength kerma constant, in unit of cGy*cm^2/hr
Λ	Dose rate constant, in unit of cm^2
$G_k(\vec{r})$	Geometry function of mass density and the distance from the radiation source. In this study the medium intensity is assumed to be 1g/ cm^3 and $G_k(\vec{r})$ is assumed to be $G_k(\vec{r}) = \frac{1}{\vec{r}^2}$.
$g(\|\vec{r}-\vec{s}_k\|)$	Radial dose function, theoretically it's $g(r) = e^{-\mu r}$, we used the TG-43 formalism in this paper
$F_k(\vec{r})$	Anisotropy function, which accounts for the anisotropy dose distribution caused by the applicator
$T_{j,k}(\vec{r},\Delta\phi_s,\Delta\theta_s)$	1, if $\vec{r}$ is inside the shield open area, 0, if shielded

2.5 Optimization methods

With the prescription dose specified by user, which in this study is 27.5 Gy, a least-squares optimization method was used to determine the emission times at each emission of all the dwell positions. The emission times were then uniformly scaled as high as possible such that none of the rectum, bladder, or sigmoid GEC-ESTRO recommended D_{2cc} values was exceeded. The objective and update function is shown in Equation 2 and 3.

$$E(\vec{w}) = \sum_{k=1}^{K} \frac{1}{T_k} \sum_{i \in Tk} [\beta^{+}{}_{k} C_{(0,\infty)}{}^{2} (d_i - d^{+}{}_{i,k}) + \beta_k{}^{-} C_{(-\infty,0)}{}^{2} (d_i - d^{-}{}_{i,k}) + \beta_k{}^{V+} C_{(0,\Delta D^{V+}{}_k)}{}^{2} (d_i - d^{V+}{}_k) + \beta_k{}^{V-} C_{(0,\Delta D^{V-}{}_k)}{}^{2} (d_i - d^{V-}{}_k)$$

Equation 2[21]. Optimization objective function

$$w^{(t+1)}{}_j = w_j{}^t \frac{\sum_{k=1}^{K} \frac{1}{T_k} \left[\beta^{+}{}_{k} \sum_{i \in I_i^+} D_{ij} d^{+}_{i,k} + \beta^{-}{}_{k} \sum_{i \in I_i^-} D_{ij} d^{-}_{i,k} + \beta^{V+}{}_{k} d_k^{V+} \sum_{i \in I_i^{V+}} D_{ij} + \beta^{V-}{}_{k} d_k^{V-} \sum_{i \in I_i^{V-}} D_{ij} \right]}{\sum_{k=1}^{K} \frac{1}{T_k} \left[\beta^{+}{}_{k} \sum_{i \in I_i^+} D_{ij} d_i + \beta^{-}{}_{k} \sum_{i \in I_i^-} D_{ij} d_i + \beta^{V+}{}_{k} \sum_{i \in I_i^{V+}} D_{ij} d_i + \beta^{V-}{}_{k} \sum_{i \in I_i^{V-}} D_{ij} d_i \right]}$$

Equation 3[21]. Optimization update equation

Table 2-3. Main variables defined in the optimization equation

$\vec{w}$	The weights of each beamlet, to be optimized, with dimension of N(dwell position)*N(emission), unit of hour
K	The number of organs considered in the optimizer
T_k	The number of voxels of the kth organ
β	The penalty factor for different situations
d_i	The prescription dose on tumor surface
$d^+_{i,k}$	The dose greater than prescription in the ith voxel, kth organ
$d^-_{i,k}$	The dose less than prescription in the ith voxel, kth organ
d^{V+}_k	The overdose threshold for dose-volume parameter
d^{V-}_k	The underdose threshold for dose-volume parameter
D_{ij}	The dose delivered to the ith voxel, by source at jth emission

2.6 Evaluation metric

With the MRI-guided TPS, the tumor volume uncertainty was reduced[20, 22] thus a higher structure related parameter, the minimal dose value for the hottest 90% tumor volume (D90), was used to evaluate the treatment quality for HR-CTV, without violation of recommendations of GEC ESTRO. The minimal dose of the hottest 2cc of OAR (D2cc) is the constraint of the OAR. The treatment time for IC, IC+IS and RSBT was calculated in our TPS to check if the increased treatment time of RSBT was clinically acceptable.

CHAPTER 3

RESULTS

3.1 D90 and treatment time statistics

The comparison of D90 and treatment time of different BT methods for 5 patients are shown in figure 3-1. For RSBT-180/IC+IS, the D90 ratio ranged from 0.66 to 1.00, with average of 0.86; the treatment time ratio ranged from 1.37 to 2.08, with average of 1.69. For RSBT-45/IC+IS, the D90 ratio ranged from 1.01 to 1.23, with the average of 1.13; the treatment time ratio ranged from 7.49 to 11.88, with the average of 9.07.

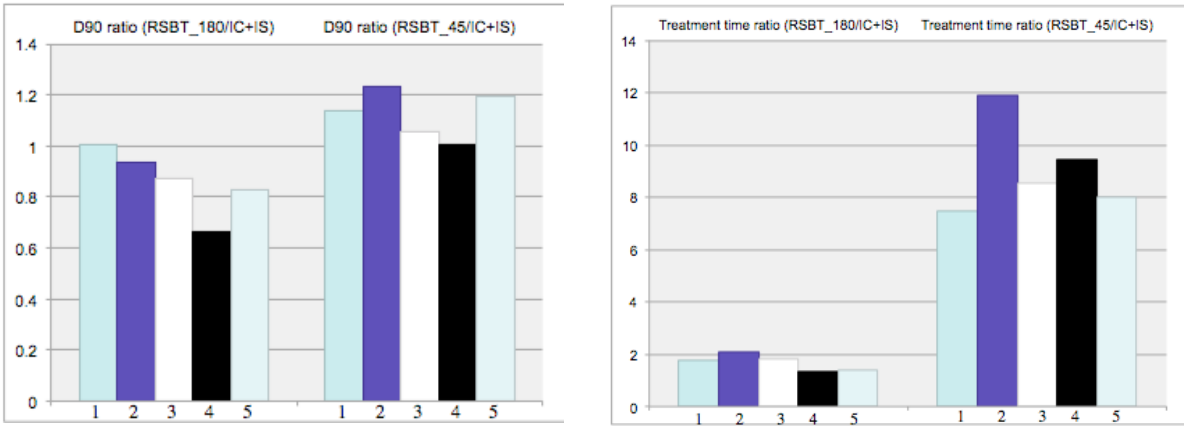

Figure 3-1. D90 and treatment time comparison between RSBT and IC+IS BT

3.2 DVH curve

The DVH for all the 5 patients are shown in figure 3-2.

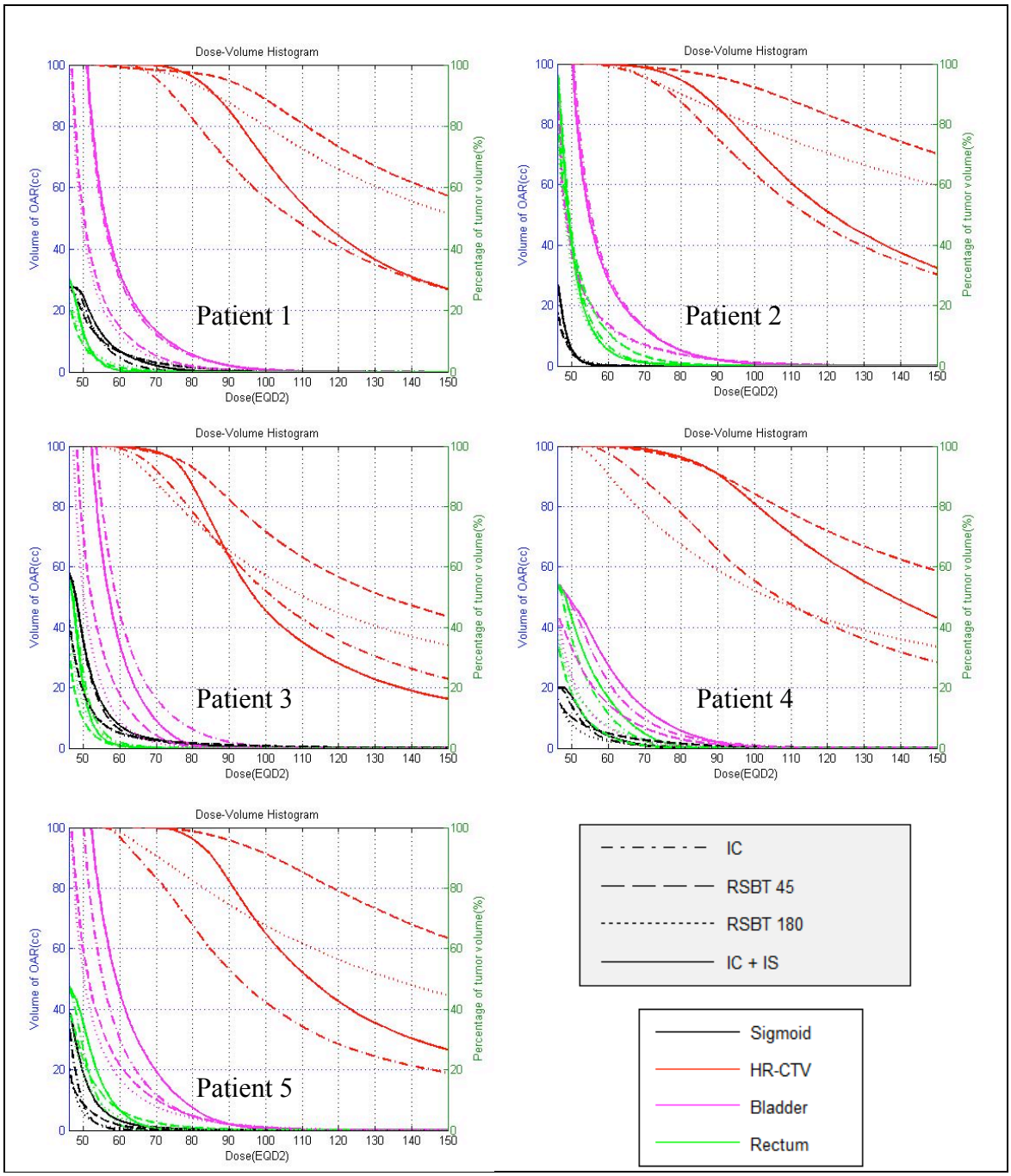

Figure 3-2. DVH of 5 patients with RSBT-180, RSBT-45, IC and IC+IS BT

3.3 Dose distribution map

The dose distribution map for the 5 patients are shown in figure 3-3.

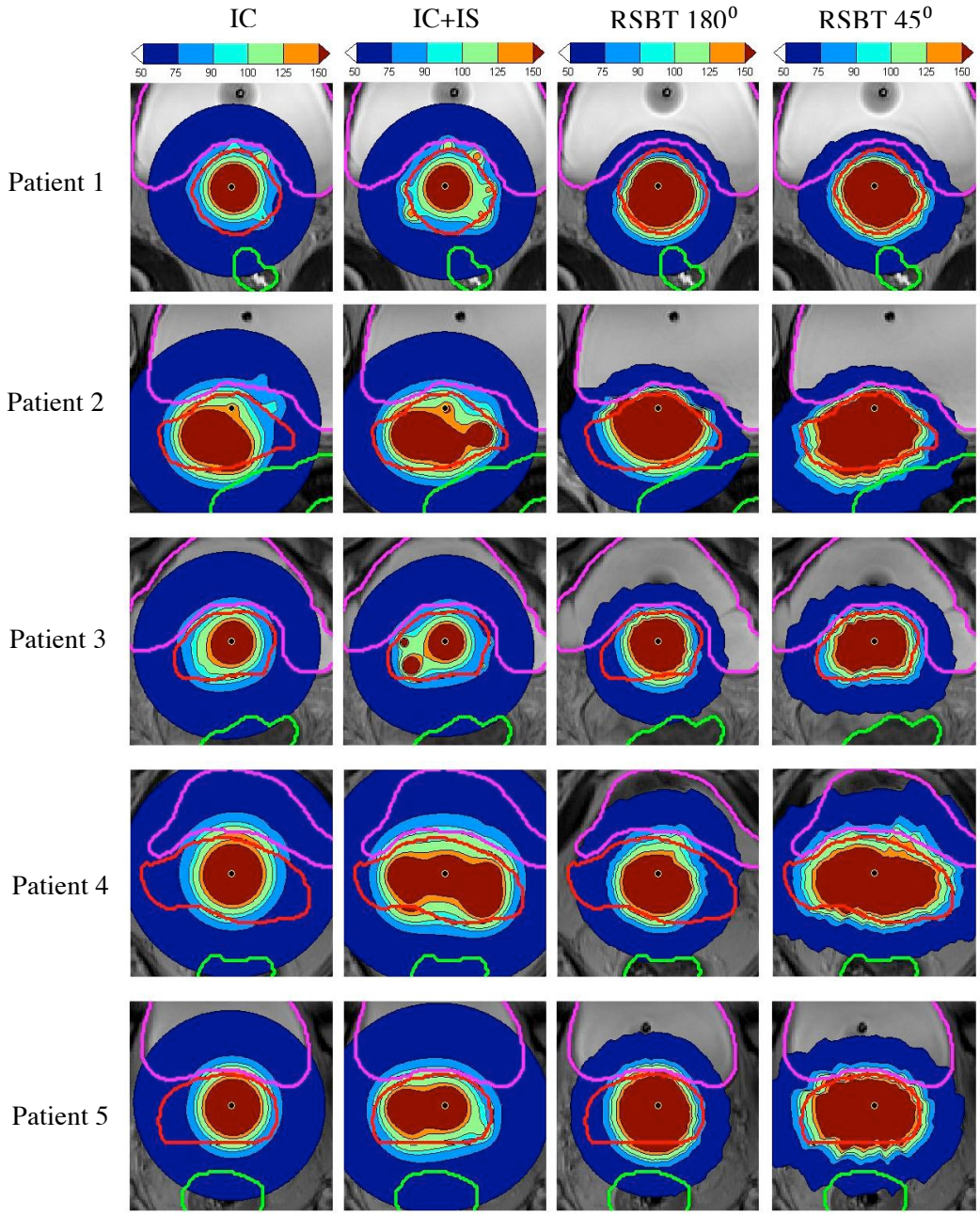

Figure 3-3. Dose distribution map for 5 patients with IC, IC+IS, RSBT-180 and RSBT-45

3.4 Effect of azimuthal angle

We applied a series shield with different azimuthal angle for patient 1 RSBT treatment. The treatment time is basically inverse linearly dependent on the azimuthal angle. There is one optimal azimuthal angle to achieve the best D90. The time-D90 curve is shown in figure 3-4.

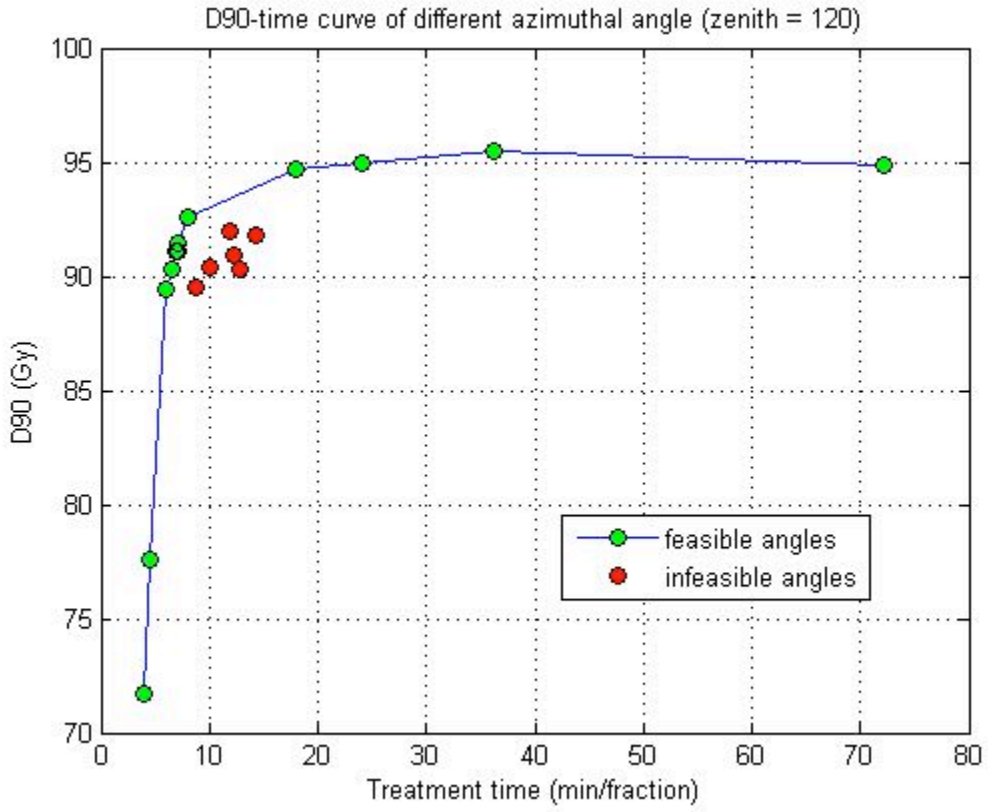

Figure 3-4. RSBT parameter selection curve. One spot represents one experiment with different azimuthal angle. Green spots represent applicable angles, and red ones represent inapplicable angles

As shown in figure 3-4, each spot means an experiment with different azimuthal but fixed zenith angle. The treatment time and D90 of different azimuthal angle consists

an outer boarder called purrito curve. The RSBT azimuthal angle should be selected right on this curve since other angle to the left of the curve means longer treatment time yet worse D90. It also can be seen that physicians could select the proper azimuthal angle based on this curve if the treatment time or D90 is with priority.

3.5 Effect of zenith angle

For patient 1, we applied different zenith angles RSBT with the constant azimuthal angle. But because of the irregular open area shape of the shield, there appeared cold area when the zenith angle is <120°. So there was not large feasible range for zenith angle and the effect of zenith angle is not clear.

CHAPTER 4

DISCUNSSION AND CONCLUSION

The treatment outcome, in terms of D90, of RS-BT is always better than intracavitary BT, which is shown in the DVH curves. The advantage of RSBT over interstitial BT is highly dependent on the tumor shape and azimuthal angle selected.

We can group patient 1 and 2 together since the D90 of RSBT with 180° azimuthal angle is at least similar to that of interstitial BT. The RSBT in these two cases will provide less invasiveness and cost acceptable extra treatment time which is less than 5 min/fraction. For patients 3,4, and 5, the RSBT-180 is less effective than IC+IS since it lowers the D90 below that of interstitial BT. We can see from figure 3-1 that the 45° RSBT will always get the best treatment outcome, the highest D90 but the extra treatment time will be very large in terms of more than 30 min/fraction.

So, for some cervical cancer shapes, RSBT with 180° azimuthal angle is a good alternative for interstitial BT, such as patient 1 and 2. However, for other irregular shapes, RSBT with finer angle such as 45° could be considered but much more treatment time is required.

The dose calculation model in our study is an approximation. We are currently using a point source model, without considering the shield transmission (<0.1%) and photon scattering. It is reasonable to assume that the dosimetric results of our study are upper bounds of the treatment outcomes of RSBT, since all these neglected factors will only cause irregular dose distribution thus decrease the D90 result.

Another problem is the escalated dose result is one BT fraction × 5. In real clinical treatment, the tumor and OAR locations and size change with time, especially for

HR-CTV. An MRI scan is thus required just prior to RSBT delivery in order to ensure organ structures of the proper sizes and extends are used for planning.

In our simulation study, the result shows RSBT could provide higher D90 than conventional IC+IS BT. More experimental work will be needed in the future to verify our computational results. Moreover, our results show that the parameter selection for RSBT is very important for different tumor shapes. An algorithm that automatically searches the best set of parameters will be helpful for making the treatment plan. (3 out of 5 is better with 45, not 60% of all patients) (tg43 method is not specific for shield)

REFERENCES

1. R. Scott Bermudez, K.H., and I-Chow Hsu, *Cervical Cancer*, in *Handbook of Evidence-based Radiation* p. 499-512.

2. Canavan, T.P. and N.R. Doshi, *Cervical cancer.* American family physician, 2000. **61**(5): p. 1369-76.

3. Kumar, V.A., Abul K.; Fausto, Nelson; & Mitchell, Richard N, ed. *Robbins Basic Pathology (8th ed.)*. 2007, Saunders Elsevier. 718-721.

4. Walboomers, J.M., et al., *Human papillomavirus is a necessary cause of invasive cervical cancer worldwide.* The Journal of pathology, 1999. **189**(1): p. 12-9.

5. Gadducci, A., et al., *Smoking habit, immune suppression, oral contraceptive use, and hormone replacement therapy use and cervical carcinogenesis: a review of the literature.* Gynecological endocrinology : the official journal of the International Society of Gynecological Endocrinology, 2011. **27**(8): p. 597-604.

6. Society, A.C., ed. *What Causes Cancer of the Cervix?* 2006.

7. Siegel, R., et al., *Cancer statistics, 2011: the impact of eliminating socioeconomic and racial disparities on premature cancer deaths.* CA: a cancer journal for clinicians, 2011. **61**(4): p. 212-36.

8. Haie-Meder, C., et al., *Recommendations from Gynaecological (GYN) GEC-ESTRO Working Group (I): concepts and terms in 3D image based 3D treatment planning in cervix cancer brachytherapy with emphasis on MRI assessment of GTV and CTV.* Radiotherapy and oncology : journal of the European Society for Therapeutic Radiology and Oncology, 2005. **74**(3): p. 235-45.

9. Potter, R., et al., *Recommendations from gynaecological (GYN) GEC ESTRO working group (II): concepts and terms in 3D image-based treatment planning in cervix cancer brachytherapy-3D dose volume parameters and aspects of 3D image-based anatomy, radiation physics, radiobiology.* Radiotherapy and oncology : journal of the European Society for Therapeutic Radiology and Oncology, 2006. **78**(1): p. 67-77.

10. Shah, A.P., et al., *Toxicity associated with bowel or bladder puncture during gynecologic interstitial brachytherapy.* International journal of radiation oncology, biology, physics, 2010. **77**(1): p. 171-9.

11. Dimopoulos, J.C., et al., *The Vienna applicator for combined intracavitary and interstitial brachytherapy of cervical cancer: clinical feasibility and preliminary results.* International journal of radiation oncology, biology, physics, 2006. **66**(1): p. 83-90.

12. Kirisits, C., et al., *The Vienna applicator for combined intracavitary and interstitial brachytherapy of cervical cancer: design, application, treatment planning, and dosimetric results.* International journal of radiation oncology, biology, physics, 2006. **65**(2): p. 624-30.

13. Syed, A.M., et al., *Long-term results of low-dose-rate interstitial-intracavitary brachytherapy in the treatment of carcinoma of the cervix.* International journal of radiation oncology, biology, physics, 2002. **54**(1): p. 67-78.

14. Lin, L., et al., *The use of directional interstitial sources to improve dosimetry in breast brachytherapy.* Medical Physics, 2008. **35**(1): p. 240-7.

15. Alain Gerbaulet, R.P.t., Christine Haie-Meder, *Cervix Carcinoma*, in *The GEC-ESTRO handbook of brachytherapy*, R.P.t. Alain Gerbaulet, Jean-Jacques Mazeron, Harm Meertens, Erik Van Limbergen, Editor 2002. p. 301-363.

16. Ebert, M.A., *Possibilities for intensity-modulated brachytherapy: technical limitations on the use of non-isotropic sources.* PHYSICS IN MEDICINE AND BIOLOGY, 2002. **47**(14): p. 2495-509.

17. Prada, P.J., et al., *High-dose-rate intensity modulated brachytherapy with external-beam radiotherapy improves local and biochemical control in patients with high-risk prostate cancer.* Clinical & translational oncology : official publication of the Federation of Spanish Oncology Societies and of the National Cancer Institute of Mexico, 2008. **10**(7): p. 415-21.

18. Shi, C., et al., *Three dimensional intensity modulated brachytherapy (IMBT): dosimetry algorithm and inverse treatment planning.* Medical Physics, 2010. **37**(7): p. 3725-37.

19. Fowler, J.F., *The linear-quadratic formula and progress in fractionated radiotherapy.* The British journal of radiology, 1989. **62**(740): p. 679-94.

20. Tanderup, K., et al., *From point A to the sculpted pear: MR image guidance significantly improves tumour dose and sparing of organs at risk in brachytherapy of cervical cancer.* Radiotherapy and oncology : journal of the European Society for Therapeutic Radiology and Oncology, 2010. **94**(2): p. 173-80.

21. Flynn, R., *A Comparison Of Intensity Modulated X-Ray Therapy To Intensity Modulated proton Therapy For the Delivery Of Non-Uniform Dose Distributions*, in *Medical physics*2007, University of Wisconsin. p. 125.

22. Hamilton, C.S. and M.A. Ebert, *Volumetric uncertainty in radiotherapy.* Clinical Oncology, 2005. **17**(6): p. 456-64.